Supporting Information

Joglekar et al. 10.1073/pnas.1718659115

SI Methods

Statement of Ethics and Regulations. PBMCs from HIV+ patients or healthy donors were collected according to protocols approved by Institutional Review Boards of Massachusetts General Hospital and California Institute of Technology. In vitro and in vivo studies were performed as per the regulations of the Institutional Biosafety Committees. All of the in vivo experiments were performed as per the regulations of the Institutional Animal Care and Use Committee.

Cell Lines and Primary Cells. HEK-293T (CRL-3216) cells and Jurkat (TIB-152) cells were obtained from American Type Culture Collection. Primary huPBMCs were obtained from University of California, Los Angeles, Center for AIDS Research Virology Core. HLA-typed huPBMCs were obtained from ReachBio LLC, Key Biologics Inc., and Fred Hutchinson Cancer Research Center Core for Excellence in Hematology. HLA type was confirmed using allele-specific sequence specific primer (SSP) assay from OneLambda. GXR-B27+ cells were maintained as described in ref. 1.

Cell-Culture Conditions and Media. HEK-293T cells were maintained in DMEM (Corning Cellgro) supplemented with 10% FBS (Sigma or Corning) and penicillin/streptomycin (Corning) (D10). Jurkat cells and GXR-B27+ cells were maintained in RPMI 1640 (Corning Cellgro) supplemented with 10% FBS and penicillin/streptomycin (R10). Primary huPBMCs were thawed in R10, coated on tissue culture-treated plates coated with 1 μg/mL anti-CD3 functional grade antibody (eBiosciences), and cultured in R10 supplemented with 1 μg/mL anti-CD28 functional grade antibody (eBiosciences) and 40 U/mL human recombinant IL-2 (Miltenyi Biosciences). All of the cells were cultured at 37 °C with 5% CO_2 (Thermo Scientific). At the end of activation, the cell population was >95% CD3+, consisting of CD4+ and CD8+ T cells (Fig. S1*D*). This cell population was used for transduction and subsequent in vitro or in vivo assays.

TCR Cloning. To clone immunodominant TCRs from B27-KK10–specific CTLs from patients, CD3+CD8+dextramer+ live singlet cells were sorted using a FACS Aria II (BD Bioscience) directly into RLT buffer supplemented with 1% β-mercaptoethanol and used for RNA extraction as per the manufacturer's instructions (Qiagen). TCRα/β chains were amplified by 5′ rapid amplification of cDNA ends as per the manufacturer's protocol (Clontech) using universal forward and gene-specific reverse primers in two rounds of PCR (Cα-outer: 5′-GTCCATAGACCTCATGTCTAGCACAG-3′, Cα-inner: 5′-ATACACATCAGAATCCTTACTTTG-3′, Cβ-outer: 5′-TGTGGCCAGGCACACCAGTGTGGCC-3′, Cβ-inner: 5′-GGTGTGGGAGATCTCTGCTTCTGA-3′). Amplification was detected by gel electrophoresis using 2% agarose gels stained with Gel Green (Biotium). Amplified PCR product was purified (Clontech) and cloned in pCR4-TOPO (Life Technologies). Presence of insert was verified using colony PCR. The PCR product was sequenced (Laragen). The Vα and Vβ families were determined using IMGT V-Quest tool (2). Upon determining the sequences, individual TCR chains were either assembled using InFusion HD cloning kit (Clontech) or synthesized using gBlocks (Integrated DNA Technologies) and cloned in pMSCV-LNGFR using NotI–BamHI (New England Biolabs) and Mighty Ligase mix (Clontech) and transformed in DH5α *Escherichia coli* (Zymo). Individual clones were confirmed by colony PCR using Accustart Taq (Quanta), and plasmids were extracted using Zyppy miniprep kit (Zymo) and verified by sequencing (Laragen). Modified versions of the TCRs encoding murine constant regions were synthesized as gBlocks (Integrated DNA Technologies) and cloned as described above.

Vector Production and Transduction. RD114-pseudotyped retroviruses encoding for the B27-KK10–specific TCRs were produced in HEK-293T cells by transient transfection of three plasmids—an MSCV-based shuttle plasmid (a gift from R. A. Morgan, NIH, Bethesda), pHIT60, and pRD114. HEK-293T cells were plated at 5×10^6 cells per 10 cm plate (Corning/BD Falcon) in D10. The cells were transfected using TransIT-293 (Mirus Bio) using the manufacturer's protocol with 7.5 μg of shuttle plasmid, 7.5 μg of pHIT60, and 5 μg of pRD114. The cell-free supernatant was harvested 72 h later and filtered through a 0.45-μm filter (EMD Millipore), aliquoted, and stored at −80 °C until further use. To transduce primary human T cells, PBMCs were first activated for 7 d as described previously. The cells were mixed with retroviral vector at 1×10^6 cells per well in 12-well nontissue culture-treated plates coated with 10 μg/mL Retronectin (Clontech) and spinfected at 1,111 *g* for 1.5 h at room temperature. The cells were incubated for 72 h posttransduction and harvested for functional assays. Jurkat cells were transduced in tissue culture-treated plates using the conditions. Replication competent virus NL4-3 (obtained through the NIH AIDS Reagent Program, Division of AIDS, NIAID, NIH from Malcolm Martin) was prepared by transient transfection of HEK-293T cells with full-length pNL4-3 using BioT (Bioland Scientific). The escape mutant R2T was generated by site-directed mutagenesis (New England Biolabs) of pNL4-3 and prepared as described above. The viral supernatant was harvested at 72 h posttransfection, filtered through a 0.45-μm filter, aliquoted, and stored at −80 °C until use. The viruses were titered with ELISA for p24 antigen (Zeptometrix) according to the manufacturer's protocol.

Antibodies, Dextramers, and Flow Cytometry. The following antibodies were used to detect expression of surface markers: anti-CD3–PE/Cy5 (clone UHCT1), anti-CD3–APC/Cy7 (clone UHCT1), anti-CD4–PE (clone OKT4), anti-CD4–PE/Cy7 (clone RPA-T4), anti-CD45–PacificBlue (clone HI30), anti-CD8–FITC (clone HIT8a), anti-TCRαβ–FITC (clone IP26), and anti-LNGFR–PE (clone ME20.4) (all from Biolegend). For intracellular staining, the following antibodies were used: anti-IFNγ–BrilliantViolet421 (clone 4S.B3) and anti-Perforin–BrilliantViolet421 (clone B-D48) (both from Biolegend). To detect surface expression of the TCR, B27-KK10-APC tetramers (NIH Tetramer core facility) or B27-KK10-APC dextramers were used (3). The staining protocol was as follows: Cells were harvested and centrifuged in 96-well plates. Cells were stained with diluted antibody and/or tetramer or dextramer mixtures in 10–50 μL PBS + 2% FBS for 20 min in the dark. For tetramer and antibody staining, the cells were stained at room temperature; for antibody staining, the cells were incubated at 4 °C. Following staining, the cells were washed once with PBS + 2% FBS and acquired on MACSQuant10 (Miltenyi). For intracellular staining, cells were first stained with antibodies against surface markers at 4 °C for 20 min and fixed using fixation buffer (Biolegend) for 20 min. The cells were then permeabilized using the Permeabilization/Wash buffer (Biolegend) three times and stained with antibodies against intracellular cytokines at room temperature for 20 min. For analyzing frequency of T cells in mouse blood, 20 μL of blood

was subjected to red blood cell lysis (Biolegend) twice, washed once with PBS + 2% FBS, and stained with 50 μL of antibody mixture at 4 °C for 20–30 min. The cells were washed once and resuspended in PBS + 2% FBS + 2% paraformaldehyde and acquired on MACSQuant 10. The data were recorded as .fcs files and analyzed on Flowjo v10 (TreeStar).

In Vivo Experiments. HuPBMC mice were constructed as described in Fig. S7*A*. Primary human T cells from an HLA-B27+ healthy donor were activated and transduced as described in *SI Methods*. Upon determining the TCR expression by flow cytometry, each arm was normalized to 2% dextramer+LNGFR+ cells by dilution with mock-transduced cells. The cells were resuspended at 10×10^6 cells per milliliter in culture medium supplemented with 40 U/mL IL-2 and kept on ice until injections. NOD/SCID/IL2R$\gamma_c^{-/-}$ mice (Jackson Laboratories), 6–8 wk old, were anesthetized using isoflurane and injected intraperitoneally with 3×10^6 cells. At 2 wk postengraftment, peripheral blood was collected from mice by retroorbital bleeding using hematocrit capillaries (Drummond Scientific) in heparinized Capiject tubes (Terumo) and analyzed by flow cytometry for the frequency of CD3+, CD4+, and CD8+ T cells (Fig. S7*B*). Plasma was collected and stored at −20 °C for viral load measurement. Mice that showed >0.5% CD3+ cells in total peripheral blood lymphocytes were used for subsequent experiments. Upon confirming human T cell engraftment, the mice were challenged with 500 ng p24 of NL4-3 by i.p. injection. Peripheral blood was collected from mice by retroorbital bleeding every week and subjected to flow cytometry analysis and plasma collection. The viral load in plasma was determined by measuring p24 antigen by ELISA (Zeptometrix) according to the manufacturer's protocol. To randomize the mice allocated to each arm, the following steps were taken: All of the mice in each experiment were numbered serially; mice were injected with transduced cells by rotating each of the experimental arms after every mouse. After the initial injection, the experimental arms were blinded, as only mouse serial numbers were followed.

Statistics. To calculate functional avidity, the maximal %IFNγ+ cell frequency, %maximal dextramer+ geometric mean fluorescence intensity, or maximal %cytotoxicity values were fitted onto a dose–response curve using least squares fit. The comparison of cross-reactivity was done using ANOVA and univariate analysis using the STATA package. To compare hCD4+ T cell frequencies in mouse models, unpaired *t* test was used. The variances of each group were compared using the *F* test. Statistical analyses were performed using GraphPad Prism (GraphPad Software).

MD Simulations. TCR homology models were next aligned to one of three ternary crystal structures (4G8G, 4G9D, 4G9F) featuring B*27:01-KK10 bound to TCRs; alignment templates were chosen based on the lowest TCR coordinate root-mean-square deviations between homology models and alignment templates. After applying disulfide bond patches, ternary complexes were solvated in TIP3P water molecules and ionized to reach biomimetic (150 mM) concentrations of Na^+ and Cl^- ions, yielding systems containing ∼100,000 atoms in total. The solvated TCRs were then minimized via steepest descent for 50,000 steps and subsequently equilibrated at 310 K with and without harmonic protein heavy atom constraints in 5-ns runs, respectively. To sample/optimize the pHLA–TCR interfaces, each ternary structure was next subjected to a simple simulated annealing procedure, whereby complexes were successively minimized across three iterations of (*i*) 10,000 steepest descent minimization steps followed by (*ii*) 10 ns of MD at slightly elevated temperature (315 K). These optimized structures were then equilibrated at 310 K for an additional 25 ns. Production simulations were seeded from final equilibrated conformations of each of the five ternary pHLA–TCR complexes and extended to 1 μs in length. All MD simulations were conducted using the NAMD 2.11 simulation package in the constant-temperature, constant-pressure ensemble (NPT); temperature and pressure were constrained at 310 K and 1 atm using a Langevin thermostat and Parrinello–Rahman barostat, respectively. Direct-space interactions were computed with a 12 Å cutoff, while long-range electrostatics were treated with the Particle Mesh Ewald method. Water molecules were constrained using the SETTLE algorithm. Representative complex structures were drawn from high population clusters derived from a hybrid *k*-means/*k*-medoids approach included in MSMBuilder 2.0. Interatomic distances between specific KK10 and TCR residues were used as a clustering metric. Rendering and energetic and SASA analyses were conducted in VMD 1.9.2. FEP calculations were completed around canonical-free and bound-state cycles using the FEP plugin in NAMD. Alchemical conformations of WT/mutant residues were generated with the VMD Mutator plugin, and binding free energy differences were calculated with the Zwanzig equation over central λ-increments of 0.04 and terminal λ-increments of descending magnitude. Alchemical moieties were treated with soft-core potentials, and electrostatic contributions were initiated at $\lambda = 0.1$. ΔΔG values were computed across 1-ns windows and averaged over five independent simulation runs in all cases.

As mentioned in the main text, the work of Ladell et al. (4) suggested an important role for a specific TCR motif (the TRBV6-5 TRBJ1-1 CDR3β) in the function of the three ternary alignment TCR templates [Protein Data Bank (PDB) ID codes 4G8G/4G9D/4G9F]. Specifically, the authors reported this specific TCR configuration resulted in resistance to the L6M escape mutation common to KK10. Though some similarities exist to the TRBV6-5 TRBJ1-1 arrangement at the N-terminal portions of our CDR3β sequences, the full motif is not present in CP27, CP7.9, FC5.5, HC25, or HC27. Despite this fact, our simulations and functional experiments both indicated robust binding to the WT and L6M versions of the KK10 peptide, in four of the five TCRs studied. CP27 represents a possible exception, though TCR function is only partially diminished in that case with the L6M mutation. It is important to emphasize that these ternary alignment complexes (4G8G, 4G9D, and 4G9F) served only as intermediaries in the model construction/optimization process; initial aligned complexes were subjected to extensive minimization, equilibration, annealing, and production MD simulation before additional analysis. Our simulation procedure produced diverse and stable KK10 epitopes with respect to TCR interaction, and our functional and simulated cross-reactivity data were in good agreement. We thus feel confident in the conclusions drawn from our simulation data. The divergent means by which control of escape mutations can evolve in TCRs (as seen here for L6M) represent an interesting topic for future study.

1. Chen H, et al. (2012) TCR clonotypes modulate the protective effect of HLA class I molecules in HIV-1 infection. *Nat Immunol* 13:691–700.
2. Brochet X, Lefranc MP, Giudicelli V (2008) IMGT/V-QUEST: The highly customized and integrated system for IG and TR standardized V-J and V-D-J sequence analysis. *Nucleic Acids Res* 36:W503–W508.
3. Bethune MT, Comin-Anduix B, Hwang Fu YH, Ribas A, Baltimore D (2017) Preparation of peptide-MHC and T-cell receptor dextramers by biotinylated dextran doping. *Biotechniques* 62:123–130.
4. Ladell K, et al. (2013) A molecular basis for the control of preimmune escape variants by HIV-specific CD8+ T cells. *Immunity* 38:425–436.

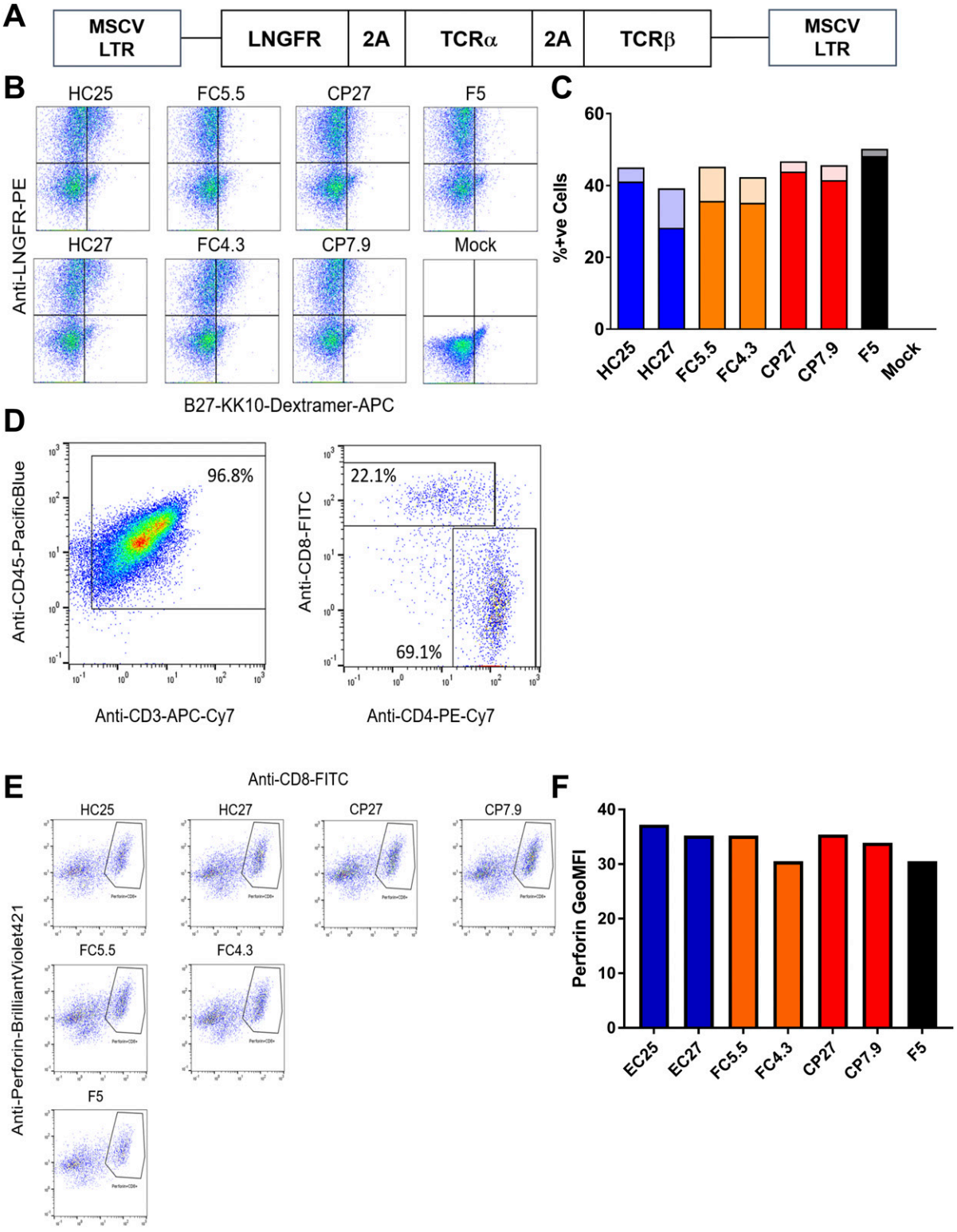

Fig. S1. Expression of B27-KK10–specific TCRs in primary T cells. (*A*) MSCV-based retroviral vector expressing LNGFR and cloned TCRs. (*B*) Measurement of transduction and TCR expression. Representative flow plots are shown. (*C*) Quantification of LNGFR+ (dark bars) and LNGFR+dextramer+ (light bars) by flow cytometry. The graph is representative of >20 experiments performed with >3 PBMC donors. (*D*) Phenotype of activated and transduced cells as measured by flow cytometry. (*E*) Flow cytometry plots showing Perforin loading in CD8+ cells as measured by flow cytometry. The cells were gated on the CD45+CD3+ LNGFR+ population and then gated on CD8+Perforin+ cells. (*F*) Intensity of Perforin staining in the Perforin+CD8+ cells among cells transduced with different TCRs is shown. Bars represent geometric mean fluorescence intensity of Perforin.

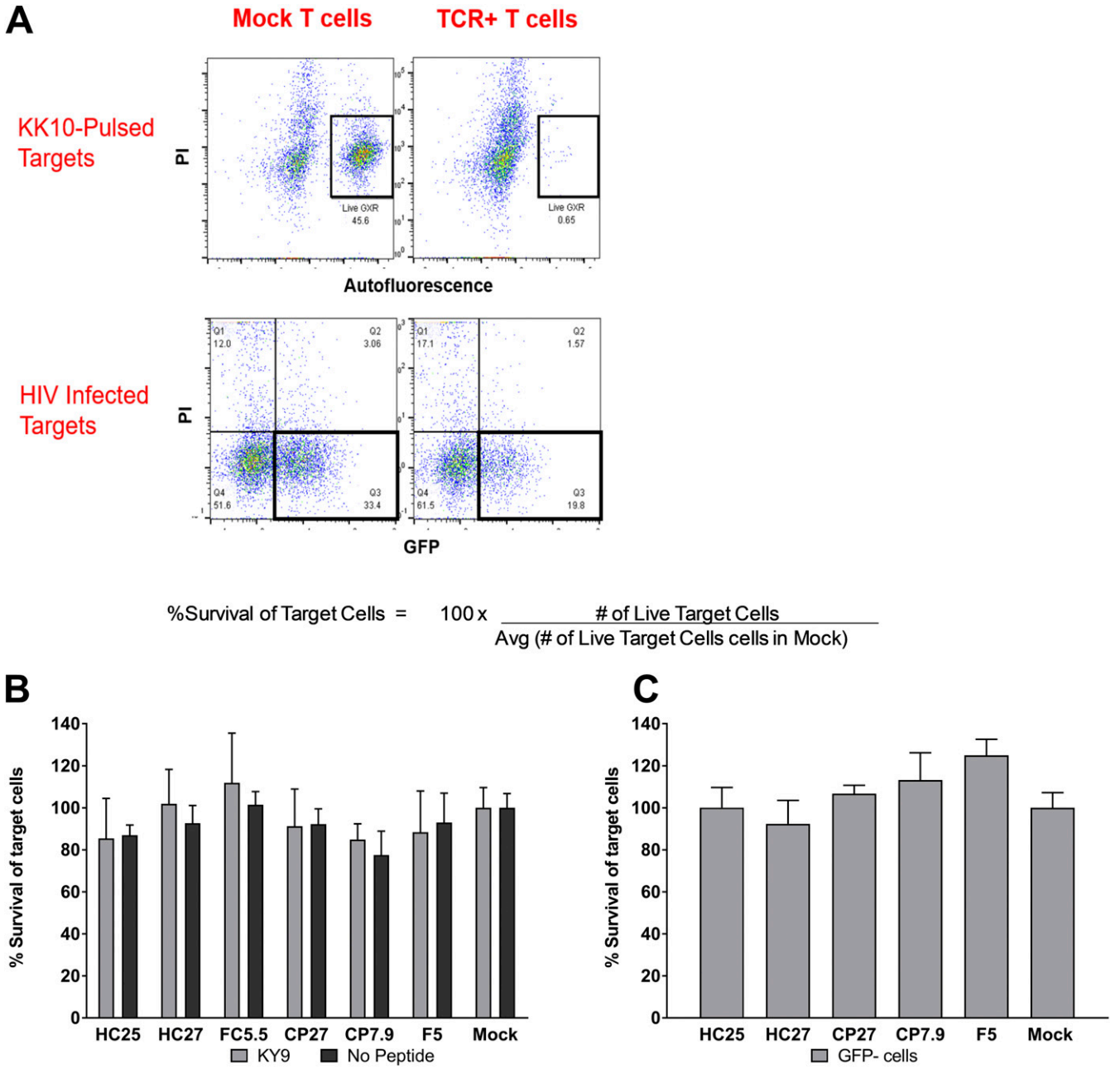

Fig. S2. Cytotoxicity assays used to quantify the ability of T cells transduced with HC–, FC–, and CP–TCRs by flow cytometry. (*A*) Representative flow cytometry plots showing cytotoxicity mediated by B27-KK10–specific TCRs and the quantification of percentage survival of target cells. (*B*) Lack of nonspecific cytotoxicity toward cells pulsed with KY9, a B27-restricted Gag epitope, or no peptide. (*C*) Lack of nonspecific cytotoxicity toward uninfected (GFP–) GXR-B27+ cells. Bars represent mean ± SEM from four technical replicates from $n = 1$.

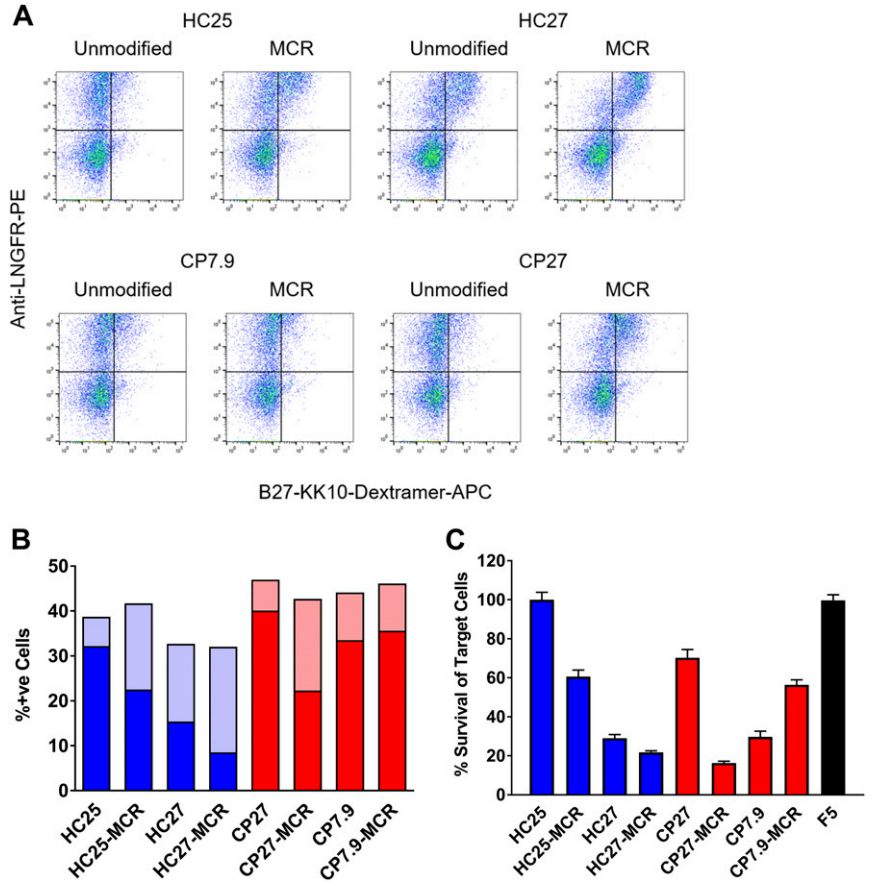

Fig. S3. Surface expression and cytotoxicity induced by murinized TCRs. (*A*) Measurement of surface TCR expression in cells transduced with unmodified or murine constant region (MCR) TCRs. Representative flow plots are shown. (*B*) Quantification of LNGFR+ (dark bars) and LNGFR+dextramer+ (light bars) by flow cytometry. (*C*) Cytotoxicity induced by transduced T cells toward GXR-B27+ cells pulsed with KK10 peptide at 24 h. The overall dextramer+ cells were not normalized in this assay.

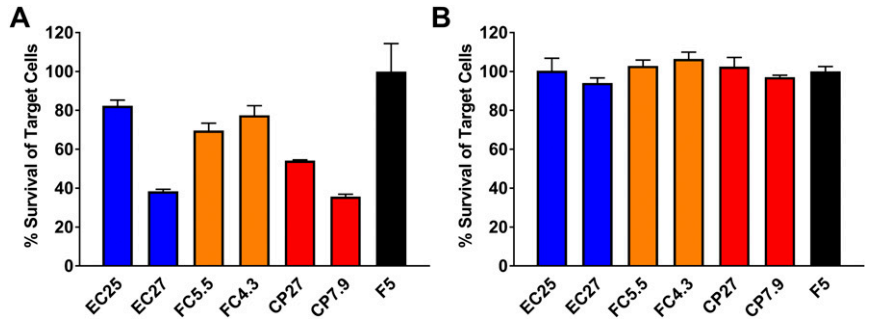

Fig. S4. Evidence for KK10 dependence of virus inhibition by TCRs. (*A*) Cytotoxicity induced by transduced T cells toward GXR-B27+ cells infected with wild-type NL4-3. (*B*) Cytotoxicity induced by transduced T cells toward GXR-B27+ cells infected with NL4-3 encoding the R2T mutant. All bars show percentage survival of target cells and represent mean ± SD from four replicates.

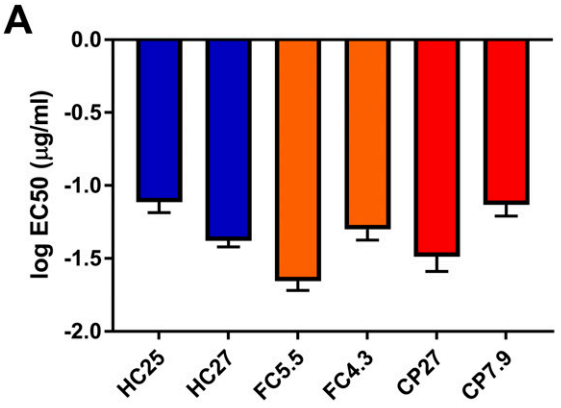

B

TCR	Log EC50	EC50 μg/ml	EC50 nM	Goodness of fit (R^2)
HC25	-1.11	0.077	61.53	0.9488
HC27	-1.38	0.042	33.43	0.9859
FC5.5	-1.66	0.022	17.66	0.9661
FC4.3	-1.3	0.050	40.09	0.9499
CP27	-1.49	0.033	26.07	0.8969
CP7.9	-1.13	0.074	59.03	0.9405

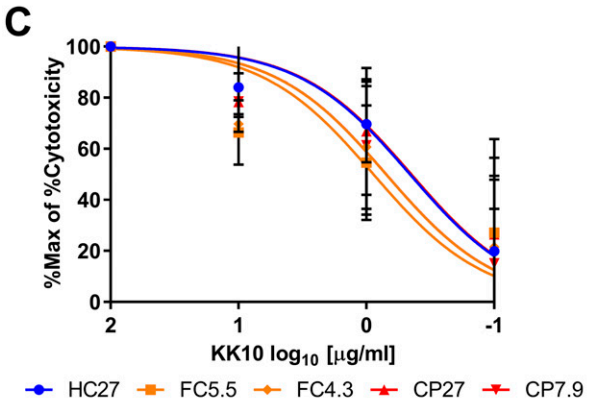

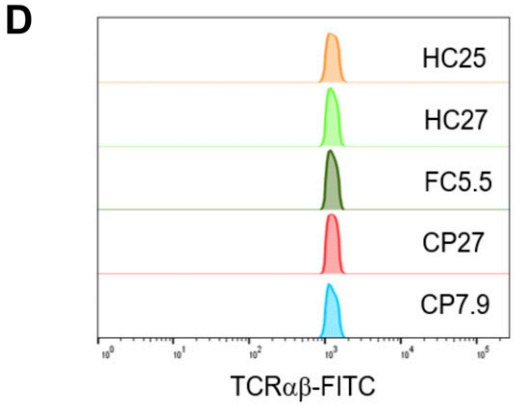

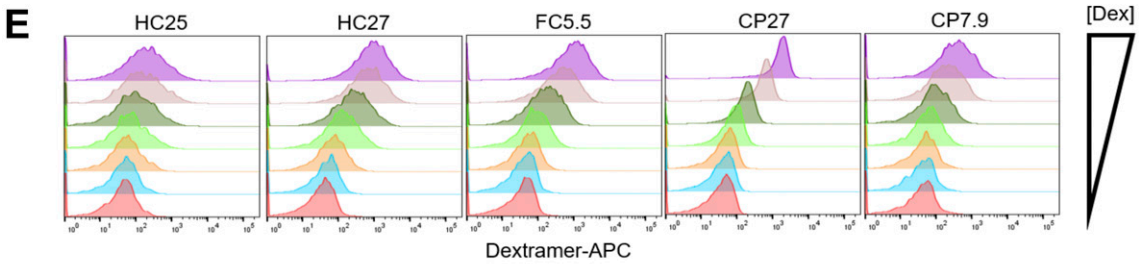

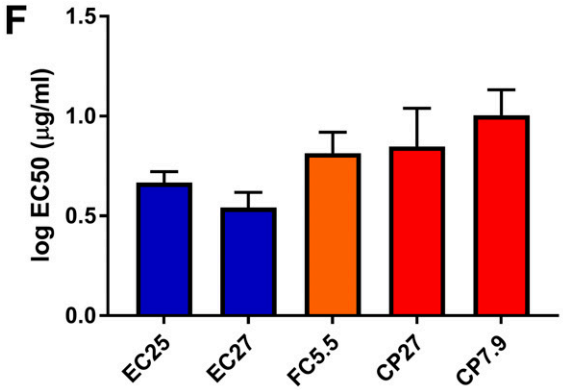

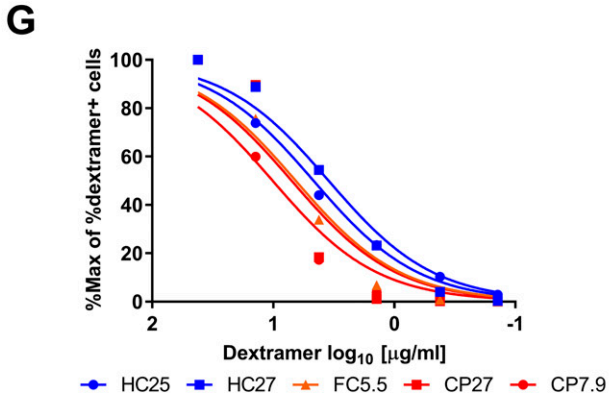

Fig. S5. Functional avidity of TCR-transduced cells. (*A*) Log EC_{50} measurements as calculated from Fig. 2*E*. The bars indicate mean ± SD from four replicates. (*B*) EC_{50} values and goodness-of-fit values for least squares fit model. (*C*) Functional avidity measurements using cytotoxicity as a readout. The lines indicate least squares fit. (*D*) The range of TCR expression used as a gate for measuring dextramer staining. (*E*) Representative flow cytometry plots showing dextramer staining as a function of reduced dextramer concentrations. (*F* and *G*) Log EC_{50} values and least squares fit for antigen sensitivity of transduced Jurkat cells, respectively.

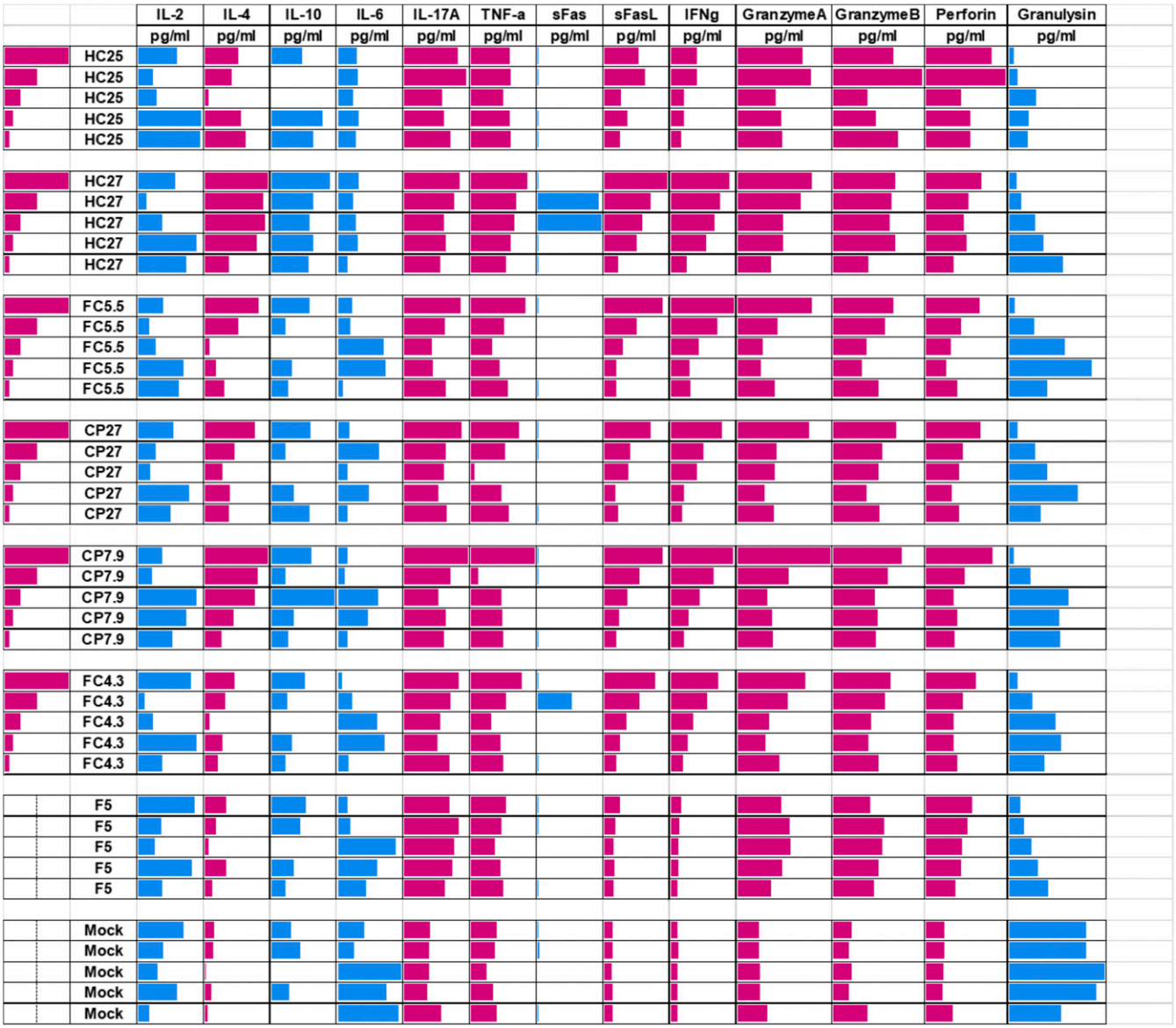

Fig. S6. Cytokine secretion induced by HC–, FC–, and CP–TCRs. The absolute values of cytokine secretion as measured by LEGENDPlex. The column on the left indicates dilution of LNGFR+dextramer+ cells in each sample. Cytokines that do not show dose dependence on LNGFR+dextramer+ cells and/or are not differentially induced by TCRs compared with F5 or mock are highlighted in blue. Cytokines that are induced by TCRs in a dose-dependent manner are highlighted in red. Cytokines highlighted here in red are shown in Fig. 2*D*.

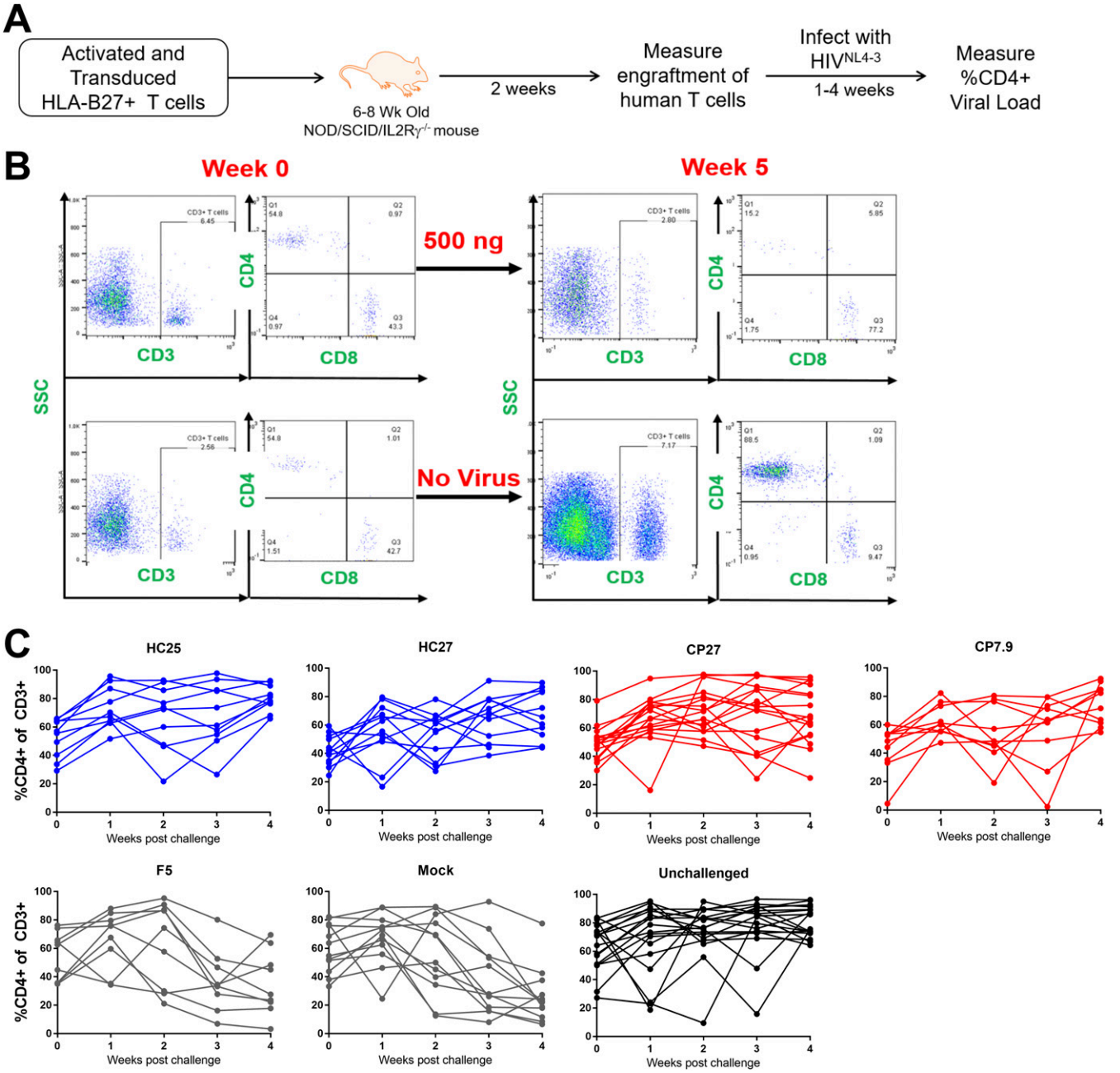

Fig. S7. HuPBMC mouse model to test the ability of T cells transduced with HC– and CP–TCRs to suppress HIV infection in vivo. (*A*) Schematic to demonstrate the establishment of the huPBMC mice and challenging them with HIV. (*B*) Representative flow cytometry plots demonstrating the gating strategy used to quantify CD3+ and CD4+ or CD8+ cells from huPBMC mice. The plots also show representative mice showing CD4+ T cell depletion upon challenge with NL4-3. (*C*) Frequency of CD4+ T cells in individual mice over 4 wk postchallenge with HIV. Data points represent individual mice from two independent experiments. The mean data composite of these mice is shown in Fig. 3*A*.

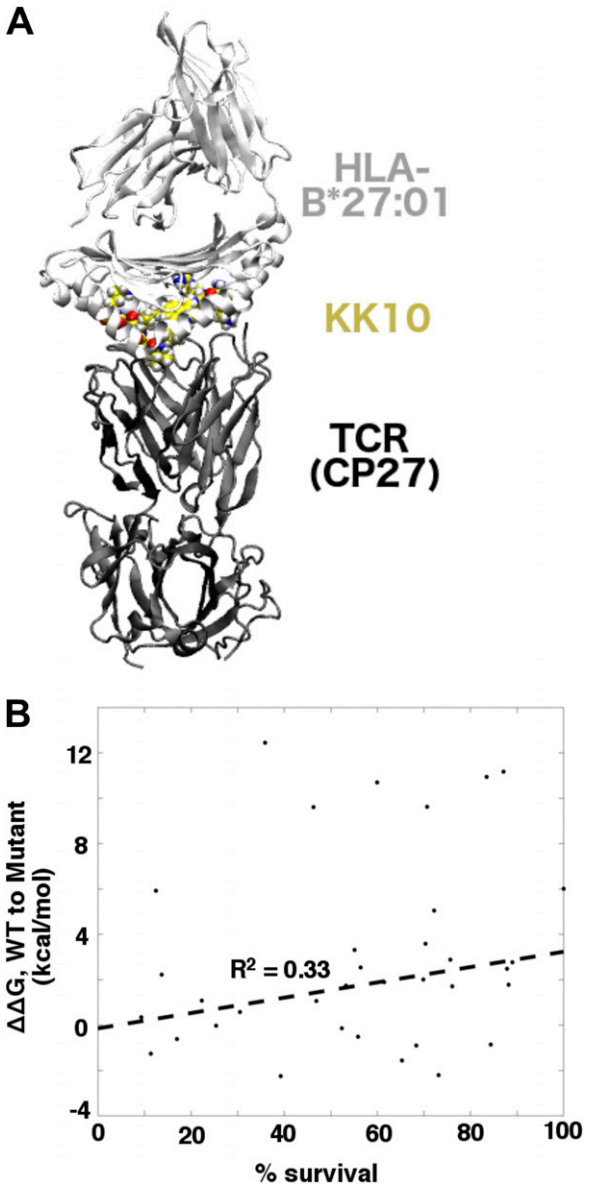

Fig. S8. MD simulations of pHLA–TCR structure and correlation with cytotoxicity. (*A*) Illustration of a ternary pHLA–TCR complex used in MD and FEP simulations, with HLA-B*27:01, wild-type KK10, and CP27 featured. (*B*) Correlation between cytotoxicity and computed binding free energy differences for KK10 escape variants. Regression analysis was completed with bisquare weights.

Table S1. Characteristics of the HCs and CPs used for this study

Subject ID	Number of viral loads, RNA copies per milliliter	CD4 count, cells per microliter	HIV diagnosis year	Birth year	Gender	Race	HIV risk	HLA class I alleles	HLA class II allele
701998 (CTR203) HC	<50	411	2006	1974	Male	Caucasian	Unknown	A*26:01, A*68:01, B*07:02, B*27:05, Cw*02:02, Cw*07:02	DPB*04:01, DPB*04:01, DQB*06:03, DQB*05:03, DRB1*13:01, DRB1*15:01
388031 HC	302	980	2004	1966	Male	Caucasian	MSM	A*11:01, A*32:01, B*27:05, B*27:05, Cw*01:02, Cw*02:02	DPB*04:01, DPB*04:01, DQB*03:02, DQB*05:01, DRB1*01:01, DRB1*04:04
529440 (BWH20) FC	<50 (on ART, VL 32,895 when started)	230 (CD4 153 when ART started)	1992	1949	Male	African American	IDU	A*01:01, A*02:06, B*08:01, B*27:05, Cw*02:02, Cw*07:01	DPB*01:01, DPB*04:01, DQB*02:01, DQB*05:03, DRB1*03:01, DRB1*14:01
708126 FC	3,520	396	2000	1974	Male	Hispanic	Occupational exposure	A*29:02, A*29:02, B*27:05, B*44:03, Cw*01:02, Cw*16:01	DPB*04:01, DPB*11:01, DQB*05:01, DQB*02:01, DRB1*01:01, DRB1*07:01
518819 (CR338) (AC160) CP	6,800	870	2004	1959	Male	Caucasian	MSM	A*0101, A*0201 B*2705, B*4403 Cw*0102, Cw*0702	DPB*04:01, DPB*11:01, DQB*05:01, DQB*06:02, DRB1*01:01, DRB1*15:01
339145 (FEN33) CP	22,094	603	2001	1959	Male	Caucasian	MSM	A*0210, A*1101, B*27:05, B*5101, Cw*01:02, Cw*16:01	DPB*04:01, DPB*04:01, DQB*0302, DQB*00,310, DRB1*04:01, DRB1*11:01

ART, antiretroviral therapy; IDU, intravenous drug user; MSM, men who have sex with men; VL, viral load.

Table S2. Characteristics of immunodominant TCRs from HCs and CPs

Patient	Subject ID	Dominant TCR	TRAV family	TRBV family	CRD3β	Frequency
HC	701998 (CTR203)	HC25	TRAV8-4*03	TRBV25	5′-CASSEADFEAF-3′	13/37
HC	388031	HC27	TRAV19	TRBV27	5′-CASSGGLPYGYT-3′	6/8
FC	529440 (BWH20)	FC5.5	TRAV22	TRBV5.5	5′-CASSSPPNTEAF-3′	12/12
FC	708126	FC4.3	TRAV14DV4	TRBV4.3	5′-CASSPGIFANEQF-3′	11/17
CP	427146 (CR338)	CP27	TRAV4	TRBV27	5′-CASSPRTGELF-3′	11/15
CP	339145 (FEN33)	CP7.9	TRAV8-4*03	TRBV7.9	5′-CASSLAGGDSYEQY-3	10/14

Vα and Vβ families, CDR3 regions, and their frequency among all Vβ chains from the immunodominant TCRs are shown. The frequency of Vβ25 for CTR203 is from the Chen et al. (1) study.

1. Chen H, et al. (2012) TCR clonotypes modulate the protective effect of HLA class I molecules in HIV-1 infection. *Nat Immunol* 13:691–700.

Table S3. Parameters for homology models

TCR	%Identity	Template	Resolution, Å	R free	Clash score	R. outliers, %
CP27_alpha	92	4oziE	3.2	0.280	6	0.7
CP27_beta	95	3vxtD	2.5	0.271	18	0.3
CP7.9_alpha	92	4gkzA	2.4	0.294	22	1.4
CP7.9_beta	95	3vxsE	1.8	0.231	5	0.1
HC25_alpha	92	1j8hD	2.4	0.245	15	0.4
HC25_beta	93	2cdfB	2.3	0.285	8	0.7
HC27_alpha	92	4jrxD	2.3	0.269	4	0.6
HC27_beta	95	3vxtB	2.5	0.271	18	0.3
FC5.5_alpha	93	2ialA	1.9	0.277	9	0.7
FC5.5_beta	85	2ntsP	2.4	0.238	16	2.2

Homology model sequence information (including template IDs, quality assessment parameters, alignments, and conservation/identity indicators) for the five TCRs featured in this work is included below. R. outliers, Ramachandran outliers.